Journal of the Korean Society of Groundwater Environment, Vol. 1, No. 2, pp. 90~99, December, 1994

Stochastic Simulation of Groundwater Flow in Heterogeneous Formations: a Virtual Setting via Realizations of Random Field

불균질지층내 지하수 유동의 확률론적 분석 : 무작위성 분포 재생을 통한 가상적 수리시험

Kang-Kun Lee (이강근)*

Abstract : Heterogeneous hydraulic conductivity in a flow domain is generated under the assumption that it is a random variable with a lognormal, spatially-correlated distribution. The hydraulic head and the conductivity in a groundwater flow system are represented as a stochastic process. The method of Monte Carlo Simulation (MCS) and the finite element method (FEM) are used to determine the statistics of the head and the logconductivity. The second moments of the head and the logconductivity indicate that the cross-covariance of the logconductivity with the head has characteristic distribution patterns depending on the properties of sources, boundary conditions, head gradients, and correlation scales. The negative cross-correlation outlines a weak-response zone where the flow system is weakly responding to a stress change in the flow domain. The stochastic approach has a potential to quantitatively delineate the zone of influence through computations of the cross-covariance distribution.

요 약 : 수리전도도의 대수값이 정규 분포를 갖고 또 공간적 상관관계를 갖는 무작위 변수라는 가정하에 지하수 유동영역 안에서 불균질한 수리전도도를 발생시켰다. 발생된 수리전도도의 거리에 따른 공분산값의 변화는 이론적으로 제시되는 변화와 잘 일치된다. 지하수위와 수리전도도는 확률론적으로 작용하는 무작위 변수들로 보고 수리전도도와 지하수위에 대한 확률 통계적 분석을 위해 몬테카를로 시뮬레이션 방법과 유한요소법을 이용하였다. 지하수위와 수리전도도의 분산값은 지하수 유동영역의 점원, 경계조건, 수위구배, 흐름방향 및 상관 거리에 따라 특징적인 분포를 보인다. 특히 수위와 수리전도도간의 공분산값이 음수인 영역은 유동 시스템의 변화에 영향을 거의 받지 않는 영역으로 볼 수 있어서 영향권의 도출과 관계시킬 수 있다.

INTRODUCTION

Over the last two decades, researchers who have been trying to understand groundwater flow and transport processes in natural geological media have begun to recognize that we do not know nearly as much as we once thought we did. Natural geological formations are generally not homogeneous nor uniformly random in terms of hydrogeologic properties such as hydraulic conductivity, specific storage, infiltration and recharge rate, etc. Heterogeneity of natural porous formations may contain multiple, nested, natural length and time scale or continuously evolving scales (Cushman, 1984; 1986; 1990).

Simulations of hydraulic-head patterns at field sites are subject to large uncertainties because of the uncertainty of input parameters. Boundaries set for flow domains may have uncertainties due to uncertain boundaries between geological units. Source-point or source-area may also have uncertainties in location and source strength. But, in most cases of groundwater flow simulation problems in the field area, hydraulic conductivity and porosity are two representative hydrogeologic parameters which have the most uncertainty in measurement and spatial distribution. In fact, conductivities within a hydrogeological unit can vary over several orders of magnitude. Most workers have found that the large variability of conductivities can be well described by a lognormal distribution (Freeze, 1975; Schwartz, 1977) and also found that log hydraulic conductivity measurements are usually autocorrelated (Garabedian *et al.*, 1991; Woodbury and Sudicky, 1992).

The present study uses the method of Monte Carlo Simulation (MCS) to simulate the hydraulic conductivity field, and the finite element method (FEM) to determine the hydraulic head field which is a known function of the hydraulic conductivity. The purpose of random conductivity simulations is

*Department of Geological Sciences, Seoul National University, Seoul, 151-172, Korea

to generate input conductivity fields for the Monte Carlo simulation of groundwater flow processes under specified physical environments. From multiple realizations of the hydraulic head field as an output, it is possible to calculate the statistics of the output and relate them to the statistics of the conductivity fields. It is also possible to elucidate statistical relationships between the output and the hydraulic parameters such as pumping rates, locations of pumping wells, recharge rates, boundary conditions, locations of boundaries, irregularity of boundaries, storativity, etc.

The Monte Carlo Simulation method is conceptually quite simple but it provides a tool to treat the hydraulic conductivity as a spatial stochastic process as illustrated by Lee *et al.* (1993) and Lee and Cushman (1993). The MCS method can be used to estimate the covariance of hydraulic head along with the head – logconductivity cross covariance which cannot be obtained by deterministic modeling.

RANDOM FIELD GENERATION

Statistical properties of conductivity data

Natural heterogeneity of geologic formations is manifest in the spatial variability of hydraulic properties which induce the randomness of the groundwater flow and transport. A random variable is a variable whose values are specified by laws of probabilities. A random function is a set of random variables corresponding to points in a unidimensional or multidimensional space. The term 'random field' is generally used in case of multidimensional space.

Hydraulic conductivity is one of typical random fields rendered from the heterogeneity of the natural porous formations. In order to get the best linear unbiased estimation of a random variable, we need to characterize the random field. A practical and quite useful characterization of a random field is the description of the random field through its mean and covariance function, i.e., its first two moments which are sufficient for the linear minimum-variance unbiased estimation. A number of researchers have characterized the spatial variability of hydraulic conductivity (K) by the covariance function of logconductivity and used stochastic methods to analyze the role of covariance plays in flow and transport (Dagan, 1989; Gelhar, 1993; Rubin and Dagan, 1987; Sun and Yeh, 1992).

The log conductivity, Y, is defined as Y=ln K , where K is the hydraulic conductivity. Y is assumed as a random variable with autocorrelated normal distribution, that is $y=N[\mu, \sigma]$ where μ is the mean and σ is the square root of the variance. The observed values of Y are commonly autocorrelated in a sense that values separated by short distance are highly correlated, and those separated by long distance are weakly correlated or not correlated. The autocorrelation function can be expressed in terms of distance. One of the most commonly used functions is the exponential model given by Jones (1990).

$$Y(d) = \exp(-d / \lambda_Y) \tag{1}$$

where λ_Y is the correlation scale and d is the distance vector. Correlation scale associated with the covariance of a stationary function is the distance between two spatial points over which random variables are considered to be uncorrelated. The present study simplifies problem that the stochastic process of logconductivity is second order stationary. Second order stationarity or wide sense stationarity is defined as: 1. The mean of a random variable is independent of position:

$$\mu(\vec{x}) = \mu \tag{2}$$

2. The covariance function between two spatial points depends only on the vector difference of the two points:

$$C(\vec{x}_1, \vec{x}_2) = C(\vec{x}_1 \quad \vec{x}_2) \tag{3}$$

The second order stationary process is anisotropic if the covariance function depends on the direction of $C(\vec{x}_1, \vec{x}_2)$, otherwise it is isotropic and the covariance function is determined by length of the vector difference $|\vec{x}_1 - \vec{x}_2|$.

The covariance function can be represented as $C(|d|, \alpha, \beta)$, where $|d|$ is the modulus of the vector d, and α and β are its longitude and latitude. The covariance function is isotropic when $C(|d|, \alpha, \beta)$ depends only on the modulus $|d|$ of the vector d. On the contrary, the covariance is anisotropic when $C(|d|, \alpha, \beta)$ is not the same in every direction. That is, the structural function $(|d|, \alpha, \beta)$ depends on the directional parameters α and β.

Representation of anisotropic covariance

A general structural function of anisotropic covariance can be made up of the nested sum of N isotropic structures:

$$C(d) = \sum_{i=1}^{N} C_i(|d_i|) \tag{4}$$

Each of the directional variabilities in Equation (4), $C_i(|d_i|)$, depends on only $|d_i|$ not on the longitude or the latitude. Each preferential direction, d_i, which composes one of isotropic structures in Equation (4) is usually known geologically. The following three preferential directions are most common as results of geological processes:

(1) Vertical direction ($|d_w|$): depositional process or surface weathering.

(2) Horizontal direction ($|d_u|$ or $|d_v|$): deposition currents in an alluvial deposit.

(3) Radial direction ($\sqrt{d_u^2+d_v^2}$): stratification. where d_u and d_v are Cartesian coordinates in the horizontal plane and d_w is a coordinate vertical to the horizontal plane. Though many preferential directions can be presented by a certain geological process or structure, the three directions will be considered in the following approach. With the preferential directions in consideration, an anisotropic covariance can be represented as:

$$C(d_u,d_v,d_w)=K_0C_0(|d|)+K_{11}C_{11}(|d_u|)+K_{12}C_{12}(|dw|)+ K_2C_2(\sqrt{d_u^2+d_v^2})+K_3C_3(|d|) \quad (5)$$

where K_0, K_{11}, K_{12}, K_2 and K_3 are positive constants and C_0, C_{11}, C_{12}, C_2 and C_3 are isotropic covariances with unit sills and a_0, a_{11}, a_{12}, a_2 and a_3 ranges.

Realization of random field

Each isotropic term in Equation (5) is taken independently to realize the corresponding random field and then all the realizations of the isotropic fields are added up for the anisotropic field. At a given point P(d) the random field z(d) is obtained by the sum of five independent random fields:

$$z(h)=z_0(d)+z_{11}(d)+z_{12}(d)+z_2(d)+z_3(d) \quad (6)$$

where $z_0(d)$ = random field with covariance $K_0(d)C_0(|d|)$

$z_{11}(d)$ = random field with covariance $K_{11}(d)C_{11}(|d_u|)$

$z_{12}(d)$ = random field with covariance $K_{12}(d)C_{12}(|d_w|)$

$z_2(d)$ = random field with covariance $K_2(d)C_2(\sqrt{d_u^2+d_v^2})$

$z_3(d)$ = random field with covariance $K_3(d)C_3(|d|)$

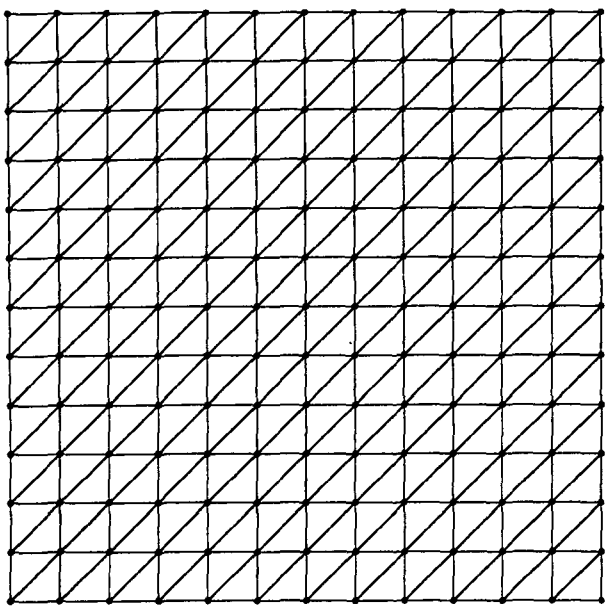

Figure 1. A square aquifer with finite elements.

VIRTUAL EXPERIMENTS

A rectangle (120 m × 120 m) is employed for the areal domain of a confined aquifer with uniform thickness and boundary conditions subject to change. The rectangular domain is divided into 288 elements as shown in Figure 1. The mean of Y is fixed at 3.5 m/day, while the variance and the correlation scale are subject to change.

Simulation of conductivity field

Many methods are available for simulation of one-dimensional realizations of a stationary stochastic process with a given covariance (Markovian generating process in Matalas (1967); Thomas and Fiering (1962); Papoulis (1965)). However, these methods are generally inapplicable to covariance functions or to functions defined over two or three dimensions.

The 'turning bands' method provides multidimensional simulations with reasonable computer costs by reducing all n-dimensional simulations to several independent one-dimensional simulations along lines which are then rotated in the n-dimensional space. The turning bands method was introduced by Matheron (1973) and it has been applied to mining geostatistics (David, 1977; Journel and Huijbregts, 1978). In the present study, the 'turning bands method' is applied to 2-dimensional simulations of the hydraulic transmissivity with given mean, variance and covariance functions. The simulation procedure for two dimensional logtransmissivity is the following:

1) Generate a sequence of normally distributed random variables u_1, u_2, u_3,..., u_n, with a mean of zero and a variance of 1.

2) Draw m lines, D_1, D_2,..., D_m, uniformly distributed over a unit sphere with the origin at O.

3) Consider a random variable Y with a zero mean and the same variance of logconductivity, σ_Y^2. Simulate Yo (Y value at the origin O) by

$$Yo=m_Y(=0.0)+\sigma_Y u_1 \quad (7)$$

where mY is the mean of Y.

4) Make nodes $X_O(D_i,), X_1,(D_i),....X_i(D_i)$ from the origin along the line Di with the same interval $\triangle l$ and make bands with the interval Δl by drawing lines passing through the mid points between nodes and perpendicular to line D_i

5) Simulate Y_i(X) at each node along D_i by

$$Y(X_i(D_i))=C_{(Y)}^{(1)}(X_{i-1}(D_i)-m_Y)+\sigma_Y[1-(C_{(Y)}^{(1)})^2]^{1/2}u_i \quad (8)$$

where $C_{(Y)}^{(1)}$ is the one-dimensional covariance function along the line D_i converted from a two-or three-dimensional

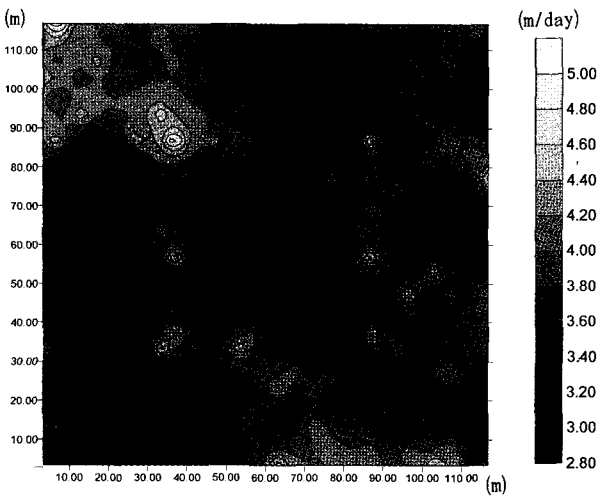

Figure 2. A realized logconductivity distribution.

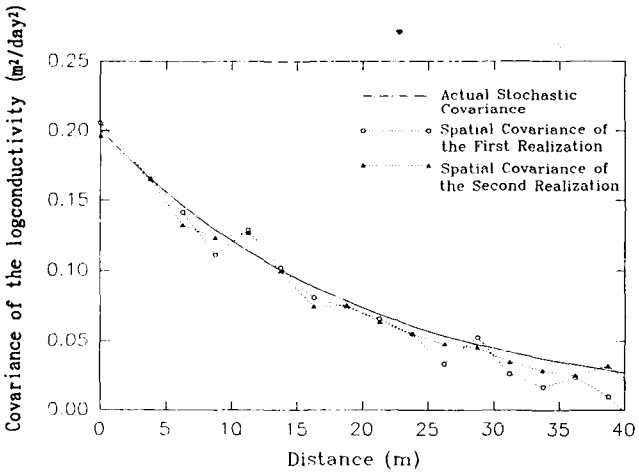

Figure 3. Spatial covariance of a realized logconductivity.

covariance. The covariance function $C^{(1)}_{(Y)}$ is not the covariance function of the two-or three-dimensional domain where the variance function is known or estimated from the sampled data. Journel and Huijbregts (1978) gave an equation to simulate the one-dimensional covariance $C^{(1)}(S)$ from the fixed three-dimensional covariance C(r) as :

$$C^{(1)}(S) = \frac{\partial}{\partial s} sC(S) \tag{9}$$

If Equation (4) is used to simulate the one-dimensional covariance function from the three-dimensional covariance function given in Equation (1), then

$$C^{(1)}(S) = (1 - |h|/\lambda_Y)\exp(-|h|/\lambda_Y) \tag{10}$$

The covariance function in Equation (10) is actually used in the simulation of $Y(X_i(D_i))$.

6) The final value of the logconductivity, y, at the point P is then obtained by taking the sum of the N contributions, i.e., N bands which encompass the point P:

$$y(X_p) = m_y + \frac{1}{\sqrt{N}}\sum_{i=1}^{N} Y(X_{pi}(D_i)) \tag{11}$$

where m_y is the mean of the logtransmissivity and Xpi is the band of the distribution line D_i which encompass the point P.

The first logconductivity realization of 100 realizations is shown in Figure 2. The sample variance of the 100 logconductivity fields exactly reproduces the specified variance within maximum deviation error of 10%. The spatial covariance of the first realization among the total 100 realizations is shown in Figure 3. The spatial covariance is computed at a series of nodes representing consecutive intervals. The spatial covariance generally matches the covariance function given for the stochastic process though the spatial covariance of a realized logconductivity distribution does not necessarily be the covariance of the random logconductivity field. In many cases, related with the ergodicity assumption, there can be a pragmatic aspect of spatial estimation associated with the need to study the statistical nature of single replicates as analogs to natural systems in which only one realization is available (Tompson *et al.*, 1989).

If a random field is wide sense stationary and generated over a domain which is substantially large in comparison with the correlation scale, then statistical estimates can be made over space for single realizations of the field. That is, the ergodic approach can be applied because the spatial statistics approach ensemble statistics as the size of the region extends to infinity.

Computation of hydraulic head field

The finite element approach using a Galerkin formulation is used to compute a head distribution from each realized conductivity field. The hydraulic head and the conductivity can be linked by solving the groundwater flow equation subject to boundary and initial conditions. A form of the partial differential equation which is assumed to govern groundwater flow in an aquifer is :

$$\nabla \bullet (\underline{K} \bullet \nabla h) + r = Ss\frac{\partial h}{\partial t} \tag{12}$$

where h=h(x,y) is the hydraulic head (dimension L), $\underline{K}$ is the conductivity tensor (dimension LT^{-1}), r=r(x,y) is the source/sink term (dimension T^{-1}), Ss is the specific storage (dimension L^{-1}), and t is the time.

Boundaries of a flow domain may be specified as one of three types of boundary conditions as follows [Javandel *et al.*, 1984; Daus and Frind, 1985]:

(1). Dirichlet (first) type boundary condition specifies head:

$$h(x,y,t) = h_o(x,y,t) \tag{13}$$

(2). Neumann (second) type boundary condition specifies normal groundwater flux:

$$(\underline{K} \bullet \nabla h) \bullet \vec{n} = q_f(x,y,t) \tag{14}$$

Standard Galerkin formulation in Cartesian coordinates is used to compute the hydraulic head distribution with each realization of the conductivity field. Firstly, the entire domain is discretized by a system of connected elements and an approximate solution $\hat{h}(x,y)$ is defined in terms of basis function as follows:

$$\hat{h} = \sum_{L=1}^{NNODE} h_L N_L(x,y) \tag{15}$$

where NNODE is the total number of nodes, $N_L(x,y)$ are the basis functions, and h_L are unknown heads at the nodes. Secondly, the approximate solution is substituted into the governing equation and the residuals of the modified governing equation weighted by NNODE basis functions is set zero when integrated over the entire domain:

$$\iint_{\Omega} \left(\nabla \bullet (\underline{K} \bullet \nabla \hat{h}) + r - Ss \frac{\partial \hat{h}}{\partial t} \right) N_L \, dxdy = 0 \tag{16}$$

Lastly, the integral equation in Eq. (16) is converted to a system of linear equations of the form:

$$[G] \left\{ \hat{h} \right\} - \{f\} - \{C\}\{h\} = \{0\} \tag{17}$$

where [G] is the global conductance matrix, {f} is a vector containing the specified fluxes, {p} is the global capacitance matrix, and $\left\{ \hat{h} \right\}$ is the vector of unknown heads. Equation (17) is solved using the iteration method.

Ensemble statistics of realizations

For each realization of y, hydraulic head at each node can be obtained by solving the boundary value problem. The collection of possible realizations of hydraulic head fields might depend on the simulation of logtransmissivity. As N, total number of logtransmissivity realizations, increases sufficiently, the following statistics will become stable :

$$\bar{h}(i) = \frac{1}{N} \sum_{j=1}^{N} h_j(i) \tag{18}$$

$$\bar{Y}(i) = \frac{1}{N} \sum_{j=1}^{N} Y_j(i) \tag{19}$$

$$R_{hh}(i) = \frac{1}{N} \sum_{j=1}^{N} (h_{(i)} - \bar{h}(i))^2 \tag{20}$$

$$R_{hY}(i) = \frac{1}{N} \sum_{j=1}^{N} (h_j(i) - \bar{h}(i))(Y_j(i) - \bar{Y}(i)) \tag{21}$$

where $\bar{Y}(i)$ and $\bar{h}(i)$ are the mean logconductivity and the mean head at node i, respectively, and $\bar{Y}_j(i)$ and $\bar{h}_j(i)$ are j-th realization of the logconductivity and head at node i. The uncertainty in the hydraulic head field is derived in the form of the mean and the covariance functions.

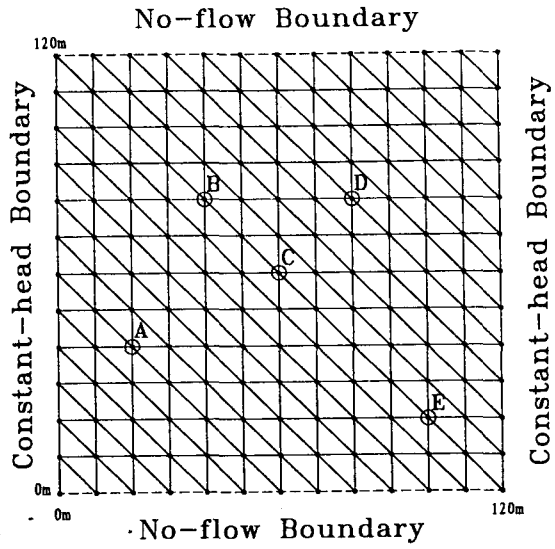

Figure 4. A flow system to compute head covariance.

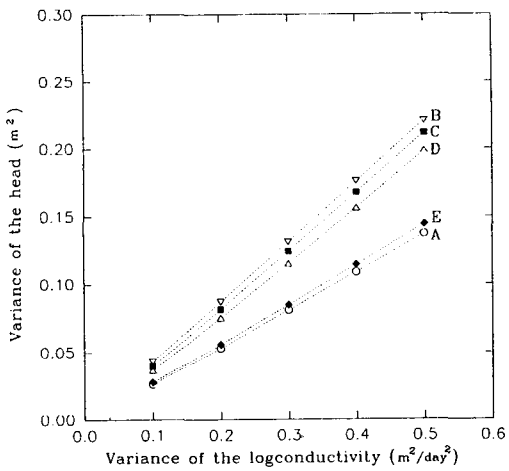

Figure 5. Head covariance versus the variance of logconductivity.

RESULTS

Effects of changes in the variance of logconductivity

Gelhar (1986) worked on an infinite aquifer and has given a result, for steady local isotropic flow,

$$\sigma_2^h \propto J^2 \sigma_Y^2 \lambda_Y^2 \tag{22}$$

where J is the mean head gradient.

Equation (22) suggests that the increment of σ_h and that of σ_Y have a linear relationship. Jones (1989) has shown a result

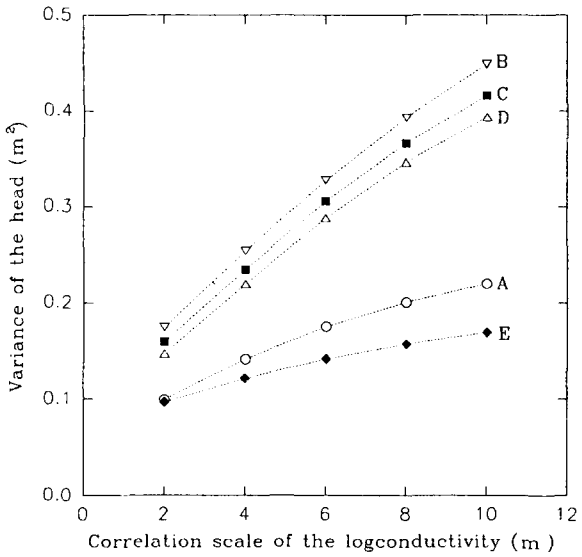

Figure 6. Head covariance versus the correlation scale of logconductivity.

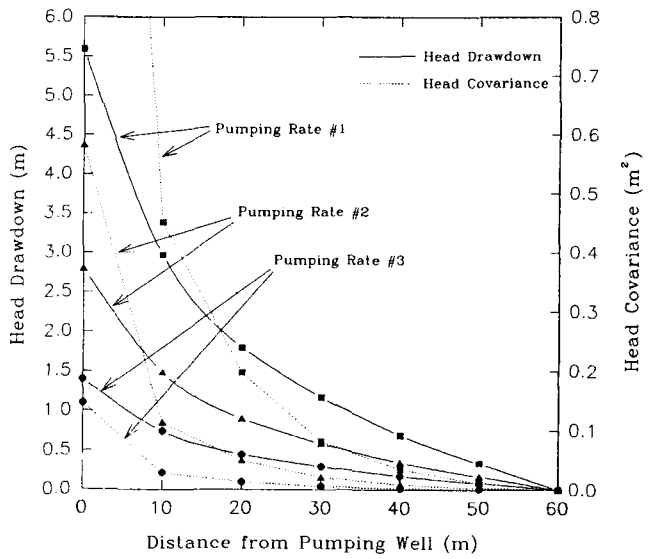

Figure 7. Head covariance with changes in pumping rate (pumping #1=50 m^3/day; #2=100 m^3/day; #3=200 m^3/day).

Table 1. Boundary condition settings to compute the head variance and the cross-covariance of the head with the logconductivity.

Setting No.	Top Boundary	Bottom Boundary	Left Boundary	Right Boundary
#1	B	B	A0	B
#2	B	C	A0	A0
#3	B	B	A0	A0
#4	B	B	B	A0
#5	B	B	A1	A0

A0 = Constant-Head Boundary (Hydraulic Head = 100 m)
A1 = Constant-Head Boundary (Hydraulic Head = 112 m)
B = No-Flow Boundary
C = Specified-Flux Boundary (Flux = 5.0 m^3/day per unit area (m^2))

which shows a linear increase in σ_h with increasing σ_Y.

A flow system shown in Figure 4 was set to compute hydraulic head and its covariance for the changes in the variance of the logconductivity. The numerical results of the present study also show a linear increase in σ_h^2 with the increase in σ_Y^2. The linear relationships appear at all nodes but $\Delta\sigma_h/\Delta\sigma_Y$ changes. The values of $\Delta\sigma_h/\Delta\sigma_Y$ around the central part of the domain are higher than those near the constant-head boundary.

The effect of changes in σ_h^2 at several selected nodes can be found in Figure 5. m_Y and λ_Y are fixed at 3.5 and 0.01, respectively, and the logtransmissivity field is generated for 100 times.

Effects of changes in the correlation scale of logconductivity

The variance of head at each node was computed for several different correlation functions by changing λ_Y. For the one-lag correlation function, λ_Y was taken as 2, 4, 6, 8 and 10. That is, the correlation function has the forms of $\sigma_Y\exp(-1/2)$, $\sigma_Y\exp(-1/4)$, etc. It was expected that the vriance of head increases as the correlation scale increases. In other words,a lpwer variance of head was expected when the conductivities in the flow domain are less correlated with each other. The variance computations of the hydraulic head with changes in correlation scale are shown in Figure 6 which shows almost linear increase in the head variance with the increase in the correlation scale.

Effects of pumping

The results of the previous numerical experiments in the present study were generated when there was no pumping. To estimate the effect of pumping, a well is located at the center node. All boundaries are set to be constant-head boundaries to remove significant modeling effects other than pumping. The variance of piezometric head has a distribution pattern similar to the head drawdown as shown in Figure 7.

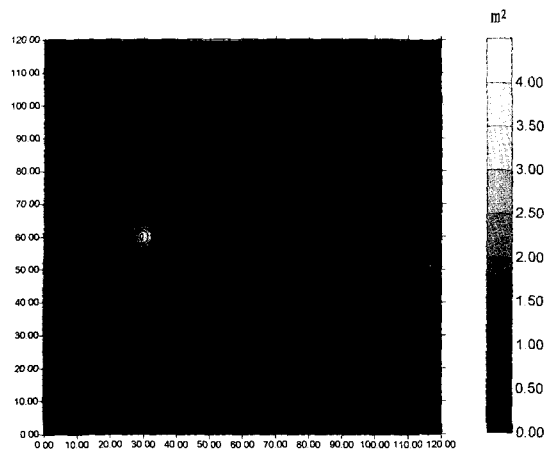

(a)

Figure 8(a). Head covariance distribution for the boundary condition setting #1.

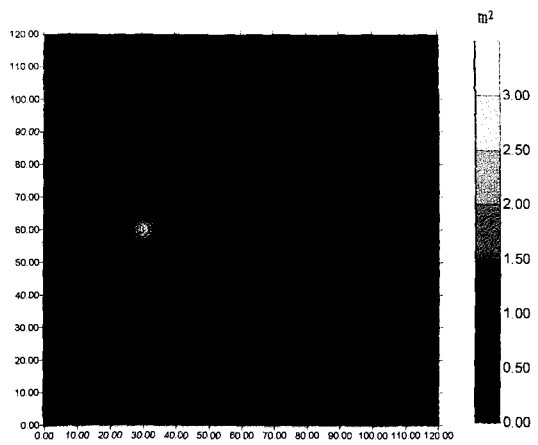

(a)

Figure 9(a). Head covariance distribution for the boundary condition setting #2.

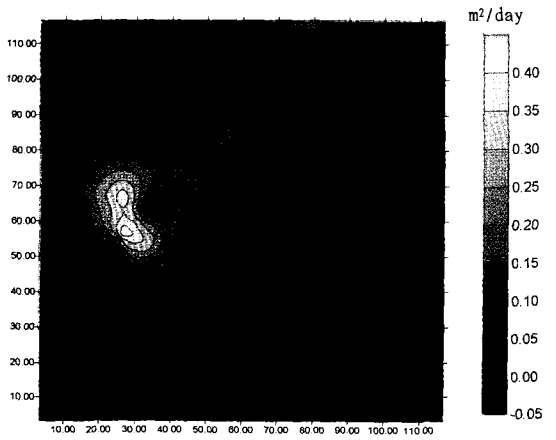

(b)

Figure 8(b). Cross-covariance of the head with the logconductivity for the boundary condition setting #1.

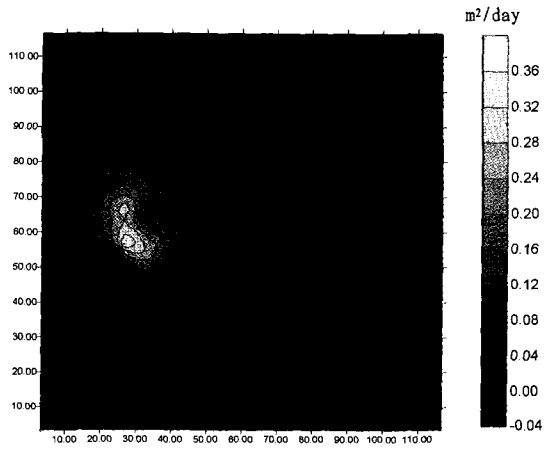

(b)

Figure 9(b). Cross-covariance of the head with the logconductivity for the boundary condition setting #2.

Three pairs of curves in Figure 7 show that the head variance increases with the increase of the pumping rate.

Effects of changes in the boundary condition and boundary head

Three types of boundaries in terms of flow conditions are used to examine the effect on the head field and its related statistics. Figures 8 – 12 show the effect of boundary conditions and boundary heads to the pumping in terms of the head variance (Figures 8(a) – 12(a)) and the cross-covariance of the head with the logconductivity (Figures 8(b) – 12(b)). A pumping well with a pumping rate 300 m^3/day is located at (30 m, 60 m) of the 120 m × 120 m flow domain. Each one of the top, the bottom, the left and the right boundaries of the rectangular flow domain is designed to have one of the specified-head, the no-flow, and the specified-flux (non – zero) boundary conditions. The flow conditions assigned to the boundaries are subject to change according to the combination of the boundary conditions to examine the change in head field associated with the boundary conditions.

Five different settings in Table 1 are used to simulate the groundwater flow. The computed head field is used for the analysis of ensemble statistics. The no-flow boundaries generally affects the head field more than the specified – head or the specified – flux boundaries. The variance of the head and the cross-covariance between the logconductivity and the head have distribution patterns influenced mostly by the no flow boundary.

The head variance has a similar distribution pattern as the drawdown trend. The cross-covariances have somewhat com-

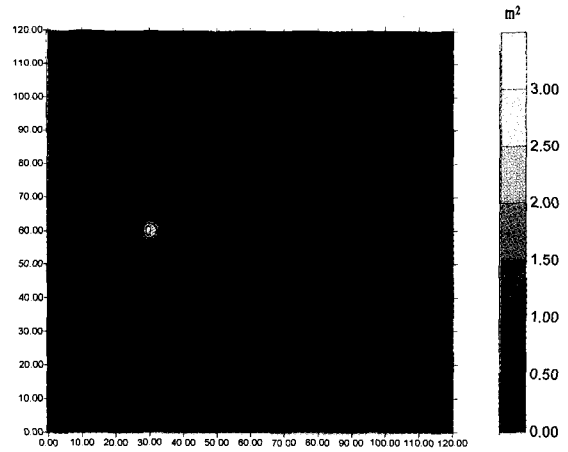

(a)

Figure 10(a). Head covariance distribution for the boundary condition setting #3.

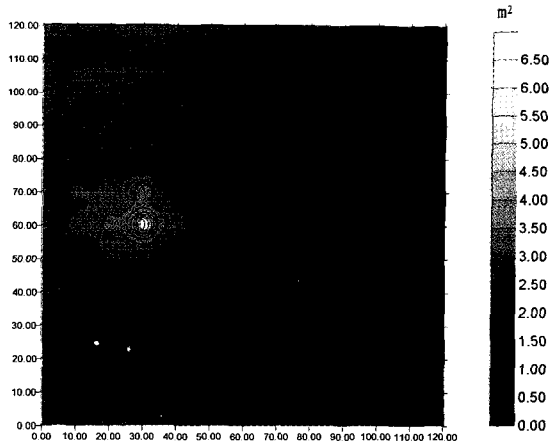

(a)

Figure 11(a). Head covariance distribution for the boundary condition setting #4.

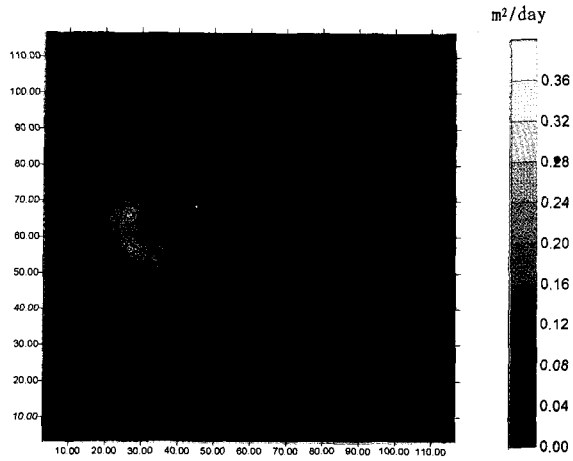

(b)

Figure 10(b). Cross-covariance of the head with the logconductivity for the boundary condition setting #3.

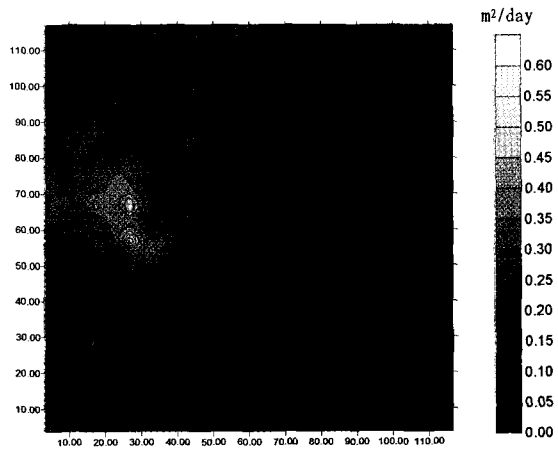

(b)

Figure 11(b). Cross-covariance of the head with the logconductivity for the boundary condition setting #4.

plicated distributions. From the fixed-head the cross-covariance tends to increase to the source of an aquifer stress (Figures 8, 9, 10, and 12). The no-flow boundary rebounds propagated stress back to the domain causing a fluctuating distribution (Figure 8). The specified-flux boundary in Figure 9 is a positive stress while the pumping well is a negative stress. These positive and negative stresses are mutually attenuated to make a fringe of negative cross-covariance along the bottom boundary (Figure 9).

Zone of influence in terms of cross-correlation

The cross-covariance of head with the logconductivity has both the positive and the negative values irregularly spread over the flow domain. The cross-covariance ϕ_{Yh} seems to have a distribution pattern in the flow domain. As Figures 8–12 show the negative (Figures 9 and 12) or infinitesimal (Figures 8, 10, and 11) value of cross-covariance is locating over the area which is weakly responding to the perturbation of the flow system caused by point sources and/or line sources such as flow boundaries.

Basically the zone of influence (ZOI) is literally meant as the zone within which head field is affected by a stress change in the hydrologic system. Theoretically there is no point or section inside the flow domain which is independent of any kind of stress change. The difference between the zone of influence and the other zone is that the head change is noticeable in the zone of influence whereas the head change, outside the zone, is an infinitesimal value or is not important compared with the magnitude of total head changes. Determination of the zone of influence is, therefore, somewhat

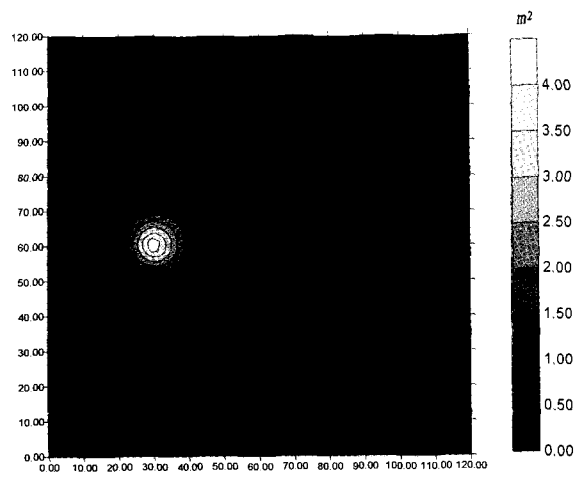

(a)

Figure 12(a). Head covariance distribution for the boundary condition setting #5.

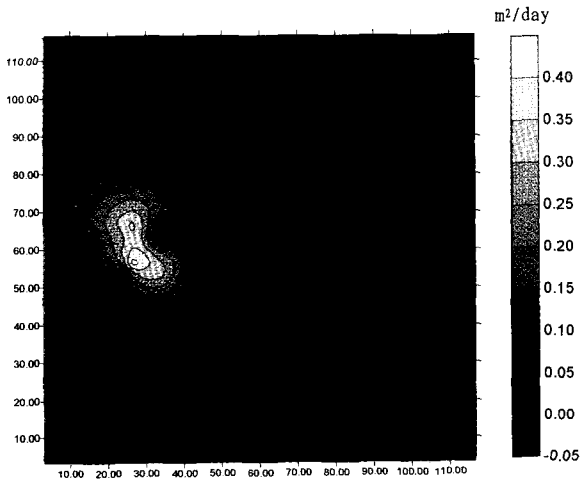

(b)

Figure 12(b). Cross-covariance of the head with the logcon ductivity for the boundary condition setting #5.

subjective unless we define the whole flow domain as the zone of influence. At the same time the determination of a finite zone under the name of zone of influence is a practical and very important in establishing a plan for the groundwater protection from contamination and exhaustion.

Practically it is not easy to exactly delineate the zone of influence when the flow domain is subject to uncertainty in hydraulic parameters. In this case the stochastic approach and its resulting ensemble statistics can be used to clearly define and to delineate the zone of influence.

CONCLUSION

The numerical results estimate the influences of logtransmissivity, correlation scale, boundary conditions and pumping to the variance of the head field. The head covariance increases with the increase in the variance of logconductivity or correlation scale. Pumping wells give a highly increased variance of the head especially in the vicinity of the wells. Therefore, the general trends of the head - variance with the changes in input parameters coincide with the results by Smith and Freeze (1979a ; b), Gelhar (1986) and Jones (1989).

The cross-covariance computations between the head and the logtransmissivity were expected to show negative values at all nodes because low values of transmissivity in a certain area tends to increase the slope of the head in the same area. However, the cross-covariance computed in several virtual settings shows values both positive and negative (Figures 9 and 12).

It is not surprising, however, because the cross - covariance of the head with the logtransmissivity shows, even in one-dimensional bounded domain, both positive and negative values as shown by Kitanidis (1989).

It seems that the zone of the negative cross - covariance is resulted by a combined effect of several factors such as the boundary condition, the geometry of the flow domain, and the distance of boundaries from the source of aquifer stresses. The exact relation between those factors with the cross-covariance is not clear yet.

The zone of negative cross - covariance or infinitesimal cross-covariance closely matches the area not significantly influenced by aquifer stresses. The stochastic approach, therefore, has a potential to be used to quantitatively delineate the zone of influence through computations of the cross - covariance distribution.

ACKNOWLEDGMENT

This study was supported by the S.N.U. Posco Research Fund (#94 - 15 - 2119).

REFERENCES

Cushman, J.H., 1984, On unifying the concepts of scale, instrumentation, and stochastics in the development of multiphase transport theory, Water Resour. Res., v.20, p.1668 - 1676.

Cushman, J.H., 1986, On measurement, scale, and scaling. Water Resour. Res., vol.22, p.129 - 134.

Cushman, J.H., 1990, Dynamics of fluids in hierarchical porous media, New York, Academic.

Dagan, G., 1989, Flow and transport in porous formations, Springer - Verlag, Berlin, 465p.

David, M., 1977, Geostatistical ore reserve estimation, Elsevier, Amsterdam.

Freeze, R., 1975, A stochastic-conceptual analysis of one-dimensional groundwater flow in nonuniform homogeneous

media, Water Resour. Res. 11, p.725 – 741.

Garabedian, S.P., LeBlanc, D.R., Gelhar, L.W. and Cella, M.A., 1991, Large – scale natural gradient tracer test in sand and gravel, Cape Cod, Massachusetts, 2, Analysis of spatial moments for a nonreactive tracer, Water Resour. Res., 27, p.911 – 924.

Gelhar, L., 1986, Stochastic subsurface hydrology from theory to applications, Water Resour. Res. 22, p. 1355 – 1455.

Gelhar, L., 1993, Stochastic subsurface hydrology, Prentice Hall, Englewood Cliffs, NJ, 390p.

Jones, L., 1989, Some results comparing Monte Carlo simulation and first order Taylor series approximation for steady groundwater flow, Stochastic Hydrol. Hydraul. 3, p. 179 – 190.

Jones, L., 1990, Explicit Monte Carlo simulation head moment estimates for stochastic confined groundwater flow, Water Resour. Res. 26, p. 1145 – 1153.

Journel, A.G. and Ch. J. Huijbregts, Mining geostatistics, 1978, Academic Press.

Kitanidis, P.K., 1989, Estimation of spatial functions and predictive groundwater modeling, Lecture Note, Stanford Univ.

Kuo, Shan S., 1972, Computer applications of numerical method, Addison Wesley Publishing Co., 415p.

Lee, K.K. and Cushman, J.H., 1993, Multiscale adaptive estimation of the conductivity field using pump test data, Stochastic Hydrology and Hydraulics, vol. 7, p. 241 – 253.

Lee, K.K., Deng, F.W. and Cushman, J.H., 1993, Multiscale adaptive estimation of the conductivity field from head and tracer data, Stochastic Hydrology and Hydraulics, vol. 7, p. 66 – 82.

Matalas, N. 1967, Mathematical assessment of synthetic hydrology, Water Resour. Res. 3, p. 937 – 945.

Matteron, G., 1973, The intrinsic random functions and their applications, Advances in Applied Probability, v. 5, p. 439 – 468.

Papoulis, A. 1965, Probability, random variables, and stochastic processes, McGraw Hill Book Co.

Rubin, Y. and Dagan, G., 1987, Stochastic identification of transmissivity and effective recharge in steady groundwater flow, 1. Theory, Water Resour. Res. 23, p.1185 – 1192.

Schwartz, F.W., 1977, Macroscopic dispersion in porous media: The controlling factors, Water Resour. Res., 13, p.743 – 752.

Smith, L. and Freeze, R.A., 1979a, Stochastic analysis of steady state groundwater flow in a bounded domain, 1, One dimensional simulations, Water Resour. Res., v.15, p.521 – 528.

Smith, L. and Freeze, R.A., 1979b, Stochastic analysis of steady state groundwater flow in a bounded domain, 2, Two – dimensional simulations, Water Resour. Res., v.15, p.1543 – 1559.

Sun, N. – Z. and Yeh, W. W – G., 1992, A stochastic inverse solution for transient groundwater flow: Parameter identification and reliability analysis, Water Resour. Res. 28, p. 3269 – 3280.

Thomas, H.A. and M. B. Fiering, 1962, Mathematical synthesis of stream flow sequences for the analysis of river basins by simulation, Chap. 12, Design of Water – Resource Systems, A. Maass et al., Harvard Univ. Press.

Tompson, A.F.B., Ababou, R. and Gelhar, L.W., 1989, Implementation of the three – dimensional turning bands random field generator, Water Resour. Res., v.25, p.2227 – 2243.

Woodbury, A.D. and Sudicky, E.A., 1992, Inversion of the Borden tracer experiment data: Investigation of stochastic moment models, Water Resour. Res., 28, p.2387 – 2398.